Low-Temperature Neutron Powder Diffraction Study of $CuCrP_2S_6$: Observation of an Ordered, Antipolar Copper Sublattice

V. Maisonneuve, V. B. Cajipe,* and C. Payen

Institut des Matériaux de Nantes, CNRS-UMR 110
2 rue de la Houssinière
44072 Nantes Cedex 03, France

Received February 24, 1993
Revised Manuscript Received April 22, 1993

Heterocharge substitution for the divalent cation M in the lamellar thiophosphates MPS_3[1] has sucessfully enlarged this family with the synthesis of $M^IM'^{III}P_2S_6$ (I–III)[2–4] and $M^I_{2x}M'^{II}_{2-x}P_2S_6$ (2I–II)[5–7] in which M^I = Ag, Cu, M'^{II} = Mn, Cd, Zn, and M'^{III} = V, Cr, In, Sc. In the $[SM_{1/3}M'_{1/3}(P_2)_{1/3}S]$ or $[S(M_{2x})_{1/3}(M'_{2-x})_{1/3}(P_2)_{1/3}S]$ layers of these materials, the metal cations and P-P pairs occupy the octahedral voids defined by the chalcogen framework. The M and M′ of the I–III and $x = 1$ 2I–II phases order in the *a*–*b* plane to form either zigzag chains or next-nearest-neighbor triangles. While the occurrence of such low-dimensional cationic arrangements has stimulated many significant investigations,[2,3,8] recent work has focused on the unusually extended shape of the Ag and Cu electronic densities around the equilibrium atomic sites in these compounds.

Smeared electronic or nuclear densities can be described either by an atom's statistical occupation of several "split" positions or its anharmonic thermal motions within fewer sites.[9] Split positions have been used in the structural determination of most MPS_3 substitution derivatives. At room temperature (RT) in $CuCrP_2S_6$ and $CuVP_2S_6$ for example, the continuous copper electronic distribution perpendicular to the layer is satisfactorily modeled in the former by two vertically disposed positions, one distinctly (Cu1) and the other slightly (Cu2) shifted from the octahedral center,[2] and in the latter by the same plus a third (Cu3) in the van der Waals (vdW) gap.[4] The structural symmetry is such that each Cu samples twice the above number of positions straddling the center of its octahedron. The incomplete occupancy of these sites may be interpreted as a static or dynamic kind of disorder. There has also been some contention regarding the existence of M_2S_6 units and metal vacancies in these I–III materials, particularly since such has been demonstrated in some 2I–II compounds,[5,6,10–12] e.g., $Cu_{0.52}Mn_{1.74}P_2S_6$.

Experiments at different temperatures (*T*) can offer some insight as to whether the RT picture represents a spatial or temporal average. An analysis of the silver distribution in $Ag_2MnP_2S_6$ at various *T* determined that the Ag site disorder within the two triangular faces of the Ag_2S_6 group is essentially static.[13] On the other hand, a study of $CuVP_2S_6$ at 20 K reported a repartitioning of Cu over only two sites per octahedron (against six at RT) but reached no conclusion about the nature of the disorder nor the occurrence of bimetallic entities.[14] In this paper, we present a neutron powder diffraction observation of an ordered Cu sublattice in $CuCrP_2S_6$ which results from an alternating single copper occupancy of upper (Cu1) and lower (Cu1′) octahedral sites at low temperature. This finding gives the first example of a structural transition in the $M^IM'^{III}P_2S_6$ series and rules out the existence of Cu···Cu pairs as well as supports a thermal hopping interpretation of the RT copper disorder in this compound.

The appearance of a new, low-*T* structure in $CuCrP_2S_6$ was first indicated by differential scanning calorimetry (DSC); a warming run revealed a well-defined peak with onset at 149 K, followed by a flatter transition between 175 and 191 K. A powder sample was then loaded into a cryostat for *T*-dependent studies on the H4S (BNL) triple-axis diffractometer operated with λ = 2.373 or 1.3585 Å radiation.[15] The Rietveld refinement[16] of the RT diffraction scan was carried out in the monoclinic *C*2/*c* space group and yielded parameters in reasonable accord with ref 2 (Figure 1a and Table I.)

The pattern measured at 64 K is clearly distinguishable from that at RT (Figure 1, λ = 1.3585 Å). First, new peaks with indexes forbidden by the *C*2/*c* space group ($h + k \neq 2n$) are observed. The C center is thus lost, i.e., the unit cell becomes primitive at low *T* (Figure 2 inset). Second, the relative intensities of several reflections carried over from the RT pattern change markedly; these compare well with those given by a powder diffraction simulation of a *C*2/*c* structure with no Cu in the near-center Cu2 position.

A refinement of the 64 K data in *P*2/*c*, the primitive space group maximally isomorphic to *C*2/*c*, suggests two positions per Cu octahedron with the sites originally related

---

(1) Brec, R. *Solid State Ionics* **1986**, *22*, 3.

(2) Colombet, P.; Leblanc, A.; Danot, M.; Rouxel, J. *J. Solid State Chem.* **1982**, *41*, 174.

(3) Lee, S. *J. Am. Chem. Soc.* **1988**, *110*, 8000 and references therein.

(4) Durand, E.; Ouvrard, G.; Evain, M.; Brec, R. *Inorg. Chem.* **1990**, *29*, 4916.

(5) Mathey, Y.; Clement, R.; Audiere, J. P.; Poizat, O.; Sourisseau, C. *Solid State Ionics* **1983**, *9–10*, 459.

(6) Mathey, Y.; Michalowicz, A.; Toffoli, P.; Vlaic, G. *Inorg. Chem.* **1984**, *23*, 897.

(7) Evain, M.; Boucher, F.; Brec, R.; Mathey, Y. *J. Solid State Chem.* **1991**, *90*, 8.

(8) Mutka, H.; Payen, C.; Molinié, P.; Soubeyroux, J. L.; Colombet, P.; Taylor, A. D. *Phys. Rev. Lett.* **1991**, *67*, 497 and references therein.

(9) Bachmann, R.; Schulz, H. *Acta. Crystallogr.* **1984**, *A40*, 668.

(10) Mathey, Y.; Mercier, H.; Michalowicz, A.; Leblanc, A. *J. Phys. Chem. Solids* **1985**, *46*, 1025.

(11) Poizat, O.; Sourisseau, C. *J. Solid State Chem.* **1985**, *59*, 371.

(12) Payen, C.; McMillan, P.; Colombet, P. *Eur. J. Solid State Inorg. Chem.* **1990**, *27*, 881.

(13) Van Der Lee, A.; Boucher, F.; Evain, M.; Brec, R. *Z. Kristallogr.* **1993**, *203*, 247.

(14) Burr, G. L.; Durand, E.; Evain, M., Brec, R. *J. Solid State Chem.*, in press.

(15) The sample was prepared as described in ref 2. We used a Perkin-Elmer DSC-4 instrument calibrated with cyclohexane and operated at 10 °C/min. Neutron diffraction experiments were done on the H4S spectrometer of the High Flux Beam Reactor at Brookhaven National Laboratory. Two monochromators were used to yield λ = 2.373 or 1.3585 Å as calibrated with CeO_2 (pyrolitic graphite (002) or silicon (220), respectively). A graphite filter, pyrolitic graphite (004) analyzer and 20′–40′–40′–20′ collimation were also in place. The sample was loaded into a 6.4 cm^3 vanadium can with Al caps; the Displex cryostat temperature was controlled with a Lakeshore DRC82C and Si diode sensors. Data were obtained at constant monitor counts in 0.1° steps; this leads to a medium angular resolution even for the normally sharper-line-width λ = 1.358 Å patterns.

(16) The neutron data were refined using the MPROF Rietveld analysis package (Murray, A. D.; Fitch, A. N. *MPROF, A Multipattern Rietveld Refinement Program for Neutron, X-ray and Synchrotron Radiation*, 1989). The pseudo-Voigt line shape with negligible asymmetry and mixing parameter was used to fit the full profile. The background was modeled with a third-order polynomial. Preferred orientation was corrected for using the March function; the Al caps' and weak $CrPS_4$ impurity peaks were accounted for with profile fits. The medium resolution of the data led to an extensive overlapping of different (*hkl*)'s so that only an overall *B* was refined and the structural parameters had relatively large estimated errors. Some interatomic distance constraints were applied to ensure a reasonable solution.

0897-4756/93/2805-0758$04.00/0

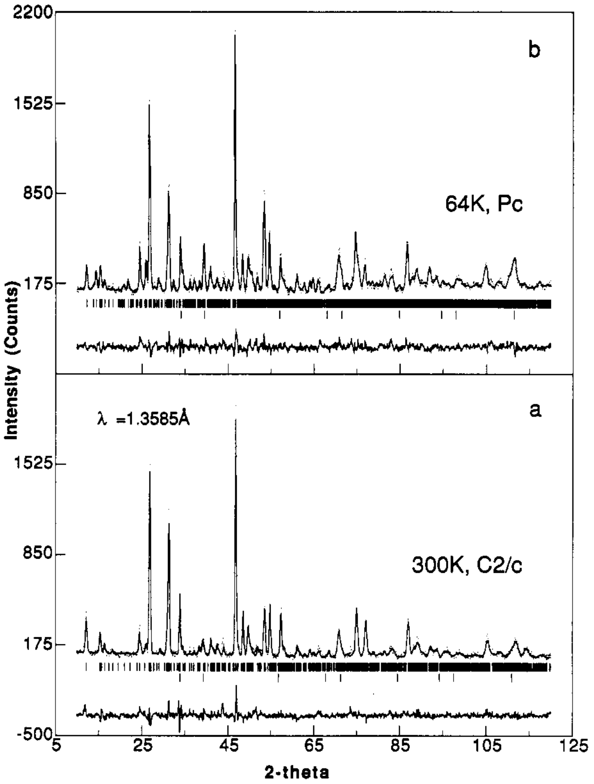

Figure 1. Experimental and calculated neutron powder diffraction patterns (λ = 1.3585 Å) for $CuCrP_2S_6$ at (a) room temperature (RT = 300 K) with a $C2/c$ structure and R_{wp} = 11.7‰ for R_{exp} = 8.0%, or $\chi^2 = 2.1$; and at (b) T = 64 K with a new, primitive and noncentrosymmetric symmetry describable by the space group Pc and refined to give R_{wp} = 10.4% for R_{exp} = 6.7%, or $\chi^2 = 2.4$. The lower row of tic marks indicates positions of Al peaks from the sample can caps.

Table I. Cell Parameters and Cu Positions at 300 and 64 K

formula $CuCrP_2S_6$		sym monoclinic		$Z = 4$	
temperature (K)		300		64	
space group		$C2/c$		Pc	
a(Å)		5.916(6)		5.935(6)	
b(Å)		10.246(2)		10.282(2)	
c(Å)		13.369(15)		13.368(13)	
β (deg)		106.74(8)		106.78(7)	
vol (Å^3)		776(2)		781(2)	
atom coordinates		x	y	z^a	τ^b
300 K	Cu1	0.058(3)	0.000(2)	0.344(2)	0.33(1)
	Cu2	0.494(11)	0.500(4)	0.270(5)	0.17(1)
64 K	Cu1	0.071(9)	0.000(3)	0.355(4)	
	Cu1′	0.441(9)	0.496(3)	0.148(4)	

[a] The octahedral center is at z = 0.25 and the basal triangles at $z \approx 0.25 \pm 0.12$. [b] τ is the site occupation ratio. With Z = 4, two 8-fold positions in $C2/c$ at 300 K imply four partially filled locations per Cu octahedron, while two 2-fold positions in Pc at 64 K yield singly occupied Cu octahedra.

by the ($^1/_2$,$^1/_2$,0) translation becoming inequivalent due to differing off-center z shifts. Fits to the stronger peaks were reasonable with this model, but the intensities for the weaker new reflections were systematically underestimated (Figure 2, λ = 2.373 Å). Not enough scattering power can thus be brought into the new Bragg planes while maintaining statistically occupied Cu sites.

A clue to the copper ordering is found in the (012) peak which would correspond to a plane defined by Cu atoms *singly* occupying their octahedra such that the z displacement of one is antiparallel to that of the atom a ($^1/_2$,$^1/_2$,0) vector away. Such a configuration with distinct and fully filled Cu1(up) and Cu1′(down) sites can be described and refined within the noncentrosymmetric space group Pc to obtain a greatly improved fit (Figure 2). A calculation applied to the 1.3585-Å pattern (Figure 1b) yielded the parameters (partly shown in Table I) used to depict the low-temperature Pc structure displayed in Figure 3.

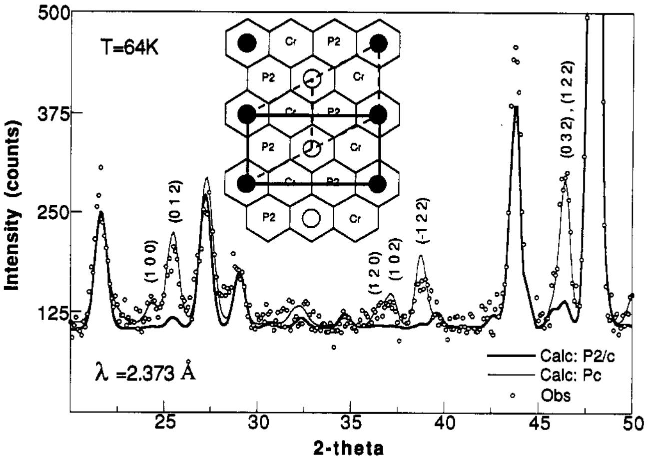

Figure 2. Comparison of the fits given by refinements of the λ = 2.373 Å pattern for $CuCrP_2S_6$ at 64 K under the monoclinic primitive space groups $P2/C$ and Pc; note how the $P2/c$ curve underestimates the new $h + k \neq 2n$ peaks. Inset: view of the a–b plane showing i) the underlying triangular arrangement of the cations (Cu represented by circles) and P–P pairs; (ii) a projection of the C-centered monoclinic unit cell which becomes primitive due to antiparallel z displacement of the originally ($^1/_2$,$^1/_2$,0)-related Cu (solid and open circles designate up and down shifts, respectively); and (iii) the doubling of the Cu sublattice cell along the monoclinic (110) which effects a triangular to "striped" phase transformation.

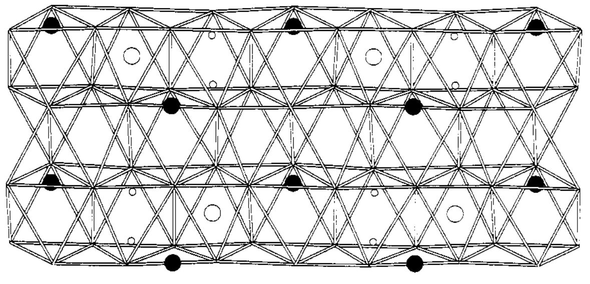

Figure 3. Perspective view of two $[SCu_{1/3}Cr_{1/3}(P_2)_{1/3}S]$ layers (separated by the vdW gap) of $CuCrP_2S_6$ at low temperature (the vertical is the c^* axis, the horizontal is the b). The S atoms (not drawn) define the framework while the Cu, Cr, and P are represented by large solid, large open, and small open circles, respectively; the octahedra of the down-shifted Cu1′ are forward of the Cu1 ones which are fully drawn (see the a–b projection in Figure 2 inset). The (012) plane is parallel to that diagonally defined by the Cu (see text).

The Cu atoms thus form an array of alternating dipoles with zero net polarization. This long-range antipolar ordering[17] conceivably lowers the intralayer Cu–Cu repulsions so that the Madelung energy associated with the two-dimensional triangular arrangement is minimized further. The observed low-T Cu sublattice, which is doubled in the (110) direction (Figure 2 inset), represents the smallest cell solution to the problem of assigning equal numbers of up- and down-shifted Cu to a triangular network's vertices.

---

(17) (a) The term "antipolar" is used here in the descriptive sense. Strictly speaking, an antipolar transition involves a vibrational mode at a Brillouin zone boundary which vanishes at the critical temperature. See: (b) Lines, M; E.; Glass, A. M. *Principles and Applications of Ferroelectrics and Related Materials*; Clarendon Press: Oxford, 1979; pp 8–15.

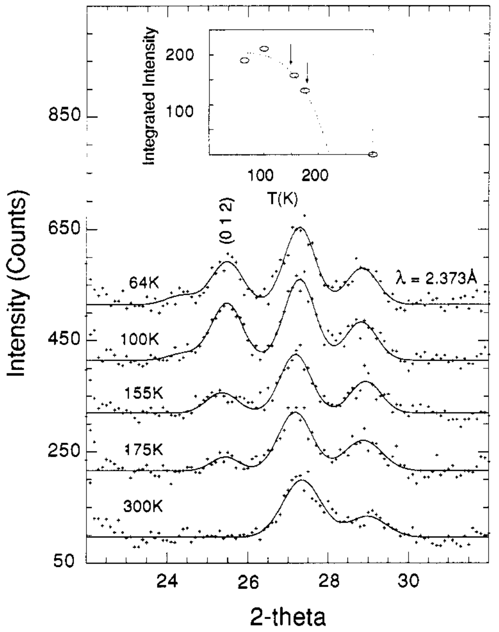

Figure 4. Short scans (λ = 2.373 Å) at various T illustrating the evolution of the (012) peak; the solid curves are Gaussian fits (≈100 counts were added each time to vertically separate the spectra). Inset: (012) integrated intensity versus T; the dotted curve is a guide to the eye and the arrows indicate the transition onset temperatures given by DSC warming runs.

At 64 K the a–b plane expands with a slight swelling of the upper or lower S-triangle of the Cu octahedral cage[18] (Figure 3), while the c parameter does not change because the antiparallel Cu disposition induces a small layer dilation which compensates for the vdW gap's low-T compression (Table I). Chalcogen stacking distortions[19] due to unequal cation sizes in $MM'P_2S_6$ are quite weak in $CuCrP_2S_6$ as in $CuVP_2S_6$ and $Ag_2MnP_2S_6$ but differ from those in the latter in their T-evolution. The discrepancy between b/a and the ideal $\sqrt{3}$ value decreases with heating in our compound rather than increases as in these other systems for which the greater filling of the vdW gap sites was invoked to explain the T-enhanced distortion.[13] This suggests that the formation of an ordered sublattice in $CuVP_2S_6$ is hindered by the low-temperature emptying of these Cu3 sites.[14]

That the copper atoms singly occupy their octahedra in the low-T structure implies that there is only one Cu per octahedron at all temperatures. This contradicts EXAFS[10] and infrared (IR)/Raman spectroscopy[11] claims that Cu_2S_6 entities exist in $CuCrP_2S_6$. These studies have previously been challenged[4,12] on grounds of improbable results for the Cr(III) coordination and Cu–S and Cr–S distance dispersions, and the disputability of the alleged matching of the $Cu_{0.52}Mn_{1.74}P_2S_6$ and $CuCrP_2S_6$ vibrational spectra. The additional structure in the 100 K IR spectrum of $CuCrP_2S_6$, absent in that of $Cu_{0.52}Mn_{1.74}P_2S_6$,[11] may in fact be ascribed to low-T distortions of the triangular faces of the Cu octahedra. Further, more recent RT EXAFS experiments on $CuCrP_2S_6$ detected no Cu···Cu pairs.[20]

The observed low-T order also renders unlikely a static disorder interpretation which would assume the occurence of exclusively Cu1 or Cu2 microdomains in $CuCrP_2S_6$: dislodging cations upon cooling from sites already "frozen" at RT is highly improbable. Moreover, the existence of a statically stable and octahedrally coordinated Cu(I) is doubtful from a stereochemical viewpoint.[21] The near-center Cu2 site should thus be regarded as a way of modeling the copper distribution rather than an equilibrium position. Recent Raman results alternatively suggest a thermally activated hopping mechanism for Cu(I) ions occupying off-center potential minima at both RT and 100 K.[12,22] In this model, the RT phase is nonpolar in a temporally rather than a spatially averaged sense and the low-T transition is of the order–disorder type.[17b]

The transition's evolution was followed with scans around the (012) peak at selected temperatures (Figure 4 with inset). The transition is already developed at 175 K and appears to have a ≈50 K span; its leveling off between 150 and 100 K gives a 0.011-eV estimate for the height of the barrier between the off-center wells. The integrated intensity's apparently smooth increase may be due to a continuous appearance and growth of ordered Cu domains. Continuity is plausible since the RT morphology is conserved while the symmetry elements are lost.[23] Our DSC results however imply two transitions in the said T range. A full discussion on the nature of the transition can be possible only after further experimentation, specifically, detailed T-dependent diffraction, vibrational and dielectrical studies.

Acknowledgment. We wish to thank D. Xie for help with the data collection, A. Jouanneaux for guidance with the refinements, and P. McMillan for insightful discussions.

Supplementary Material Available: Tables of all atomic coordinates and main interatomic distances at 64 K (2 pages). Ordering information is given on any current masthead page.

---

(18) The up-and-down pattern may also be thought of as a steric effect accomodating these deformations.

(19) Ouvrard, G.; Brec, R. *Eur. J. Solid State Inorg. Chem.* **1990**, *27*, 477.

(20) Prouzet, E., private communication.

(21) The $3d^{10}s^0$ Cu(I) electronic configuration favors a linear or tetrahedral coordination, the latter being common in sulfides (see: Wells, A. F. *Structural Inorganic Chemistry*; Oxford University Press: Oxford, 1984; p 1142). Although a tetrahedral environment is possible within and between the layers, the stable MPS_3 structure apparently forces the Cu(I) into S-octahedra within which these stabilize at off-center locations.

(22) The non-observation of soft modes in $CuCrP_2S_6$ (Payen, C.; McMillan, P., unpublished results) is consistent with this: instead of small quasi-harmonic motion about a mean position, the Cu undergoes large-amplitude thermal hopping between the wells flanking the central site. These motions diminish with cooling so the cations eventually freeze into single sites.

(23) Rao, C. N. R.; Rao, K. J. *Phase Transitions in Solids*; McGraw-Hill: New York, 1978; p 174.